
Article:
Luo, G., Hu, X., Bowman, E.T. et al. (2017) Stability evaluation and prediction of the Dongla reactivated ancient landslide as well as emergency mitigation for the Dongla Bridge. Landslides. ISSN: 1612-510X

https://doi.org/10.1007/s10346-017-0796-9

Stability evaluation and prediction of the Dongla reactivated ancient landslide as well as emergency mitigation for the Dongla Bridge

Gang Luo[1], Xiewen Hu[1,2], E T Bowman[3], Jingxuan Liang[1]

1 *Department of Geological Engineering, Faculty of Geosciences and Environmental Engineering, Southwest Jiaotong University, Chengdu 610031, China.*

2 *State-province Joint Engineering Laboratory of Spatial Information Technology for High-Speed Railway Safety, Chengdu, Sichuan, 610031，China*

3 *Department of Civil and Structural Engineering, Faculty of Engineering, University of Sheffield, Sheffield, S1 3JD, United Kingdom.*

Corresponding author: Gang Luo (E-mail: luogang@home.swjtu.edu.cn).

Other authors: Xiewen Hu: e-mail: huxiewen@163.com; E T Bowman: e.bowman@sheffield.ac.uk; Jingxuan Liang: 952914714@qq.com

Abstract: The Dongla Bridge, Muli County, China, is a key access road between counties in Sichuan province and the only traffic facility for an important 500 kV electricity substation which provides power to nearby counties. In June 2011, during the bridge construction, an unknown landslide, subsequently named the Dongla Ancient Landslide (DAL), was encountered. Local reactivation of a portion of the DAL, termed the Dongla Reactivated Landslide (DRL), was indicated by evident ground deformation at the Dongla Bridge. In spite of this, transportation of some heavy electrical equipment to the substation was scheduled on 9 May 2013. So to guarantee the stability and security of the bridge became a primary emergency task. Detailed field investigations of the landslide occurrence, monitoring and emergency mitigation construction were carried out in the period between 2011 and 2014. This resulted in a temporary stabilization of the revived landslide and ensured the timely transportation of the heavy electrical equipment. It is thought that the revival mechanism of the DRL is creep – translational sliding, and was mainly triggered by artificial slope-cutting, but also influenced by precipitation, river erosion and man-made activities in the form of small-scale mining operations. Following complete failure of the DRL, the probability of landslide-dam and dam breach is proved to be small by Risk Analyses. This paper can provide an insight into the problems associated with the interaction between the human structures and landslide instabilities.

Key words: Dongla Reactivated Landslide; failure mechanism; stability evaluation; landslide emergency mitigation

1. Introduction

The Dongla Reactivated Landslide (DRL) is located in the Shuiluo River, 10 km upstream from Shuiluo village, and 100 km upstream from Muli county of Sichuan province, China. It is located within an impoverished and sparsely populated mountainous region, connected previously by only poor-quality roads (Figure 1). Hydropower has recently been developed in this area and in order to provide a vital road link to a 500kV electricity substation as well as access to other counties, the 134 m long Dongla Bridge which crosses the Shuilou River, was completed in 2011 at the cost of 8 million Yuan. Unfortunately, due to inadequate geological exploration, the bridge abutment was located within a pre-existing ancient landslide (Figure 2), known here as the Dongla Ancient Landslide (DAL).

The approximately 6 million m^3 DRL was activated in June 2011 within the larger DAL which has an estimated total volume of 2 billion m^3. After several periods of torrential rainfall in June 2011, deformation of the ground and bridge, including cracks, subsidence and dislocation became progressively visible. This condition posed a serious threat to the serviceability of the bridge and the local inhabitants.

The timely provision of electricity supply to this remote region was considered vital for the successful completion of the hydropower station. That depended on the transportation of heavy electrical equipment by a specific date (9th May 2013). Therefore, instead of focusing on mitigation of the DRL itself, the protection of Dongla Bridge was considered to be more important for the main stakeholder - China Power Engineering Consulting (Group) Corporation. Based on previous geological experience, if

effective remediation was not carried out to reduce the continuous displacement of the landslide, the bridge would be destroyed and the river would be dammed. Authorized by the stakeholder, detailed geological investigation of the failure mechanism, displacement monitoring, and emergency mitigation, were conducted successively from December 2012 to April 2014.

This paper discusses the measures taken, and how this type of problem can be tackled in a broader context – specifically focusing on the importance of ground investigation and monitoring to understand the mechanisms of movement of a particular slope and therefore, how such movement can be mitigated.

2. Geological setting of research area

2.1 Geomorphology

The drainage basin of the Shuiluo River is located at the transition area between the Qinghai-Tibet and Yunnan-Guizhou Plateaus, in the eastern Hengduan Mountains. The geomorphological pattern is an erosion terrain inclining from north to south with complicated geomorphic types. Due to deep incision cut by the river, the stretch where the DRL developed is 50 m - 60 m wide with a characteristic "V" shaped valley and 40° ~ 50° bank slopes (Figure 2).

2.2 Hydrology

Precipitation is mainly in the summer rainy season (May to October), when each year floods from upstream inundate the toe of bank slopes over a period of three to five days (He, 2005). The pore-phreatic water is significantly influenced by the water level of the Shuiluo River, although no perched water table develops on the slope surface.

2.3 Neotectonic activity and seismicity

The research region is tectonically active because of its location at the margin of the Tibetan Plateau,

where intensive intermittent uplift has resulted in a distinctive topographical contrast with the plateau and lower basins, high mountains and deeply incised valleys (Huang, 2015). From 1991 to present, around 30 earthquakes with seismic intensities of Modified Mercalli scale MM V or larger have been recorded (He, 2005). According to National Seismic Standardization Technical Committee (2015), the typical seismic intensities in Shuiluo Village area are MM V to MM VII, and the peak ground acceleration (PGA) is 0.10 g with a response spectrum period of 0.45 s.

2.4 Stratum lithology

The Dongla Ancient Landslide, within which the DRL located, is situated on the lower part of the right bank slope. Through field investigation, lithologies belong to the Quaternary and the Triassic was confirmed. The Quaternary part mainly consists of residual, alluvial, diluvial and colluvial deposits, as well as reworked landslide deposits that consist of angular tuff blocks, fine gravel, sand, silt and clay with weak mechanical strength. The grain-size distribution of the surficial deposit was estimated by visual observation (Table 1). The Triassic part (T_1L) forms outwardly tilting bedrock (N42°-58°W/NW ∠50-68°). The outcrops are sporadically distributed in the slope surface and the bottom of ditches.

2.5 Anthropogenic activity

During the field investigation, more than 50 gold mining pits spread randomly over the bank slopes were found. According to the local inhabitants, after a gold-bearing layer in the bank slopes was found, from 1990 to 2000, a large number of illegal gold mining activities were conducted on the slope, which caused great damage to the vegetation and soil conservation. Because of the subsequent intervention of the government and the decrease of gold reserves, the mining gradually stopped. Although the ecology recovered to some extent and the vegetation coverage increased greatly, a great deal of consequences remained. As the support timbers in caves and pits in the slope weathered and rotted, the ground tended

to subside and slowly crack. Subsequently, the newly formed cracks provided direct conduits for precipitation to get into the landslide. Although the influence is difficult to be quantified precisely, the intricate net of mining tunnels is considered to have contributed to the destabilization of the slope.

In addition, the engineering excavation for the new-built ancillary road and bridge construction (Figures 3 - 5) undercut the toe of slope, resulting in a reduction in the stabilizing force. The influence of this excavation is discussed in detail in Section 7 and 8.

3. Field survey and brief history of the DAL

A large number of ancient landslides exist in the mountain canyons of Sichuan province due to tectonic activities (He 2005; Cui et al. 2008). Their characteristics are crescentic-shaped headscarps, gentle multi-terraces and steeply sloping toes that stretch into rivers (Wang et al. 2003; He 2005; Dong et al. 2014). Topographically, the 1500 m long and 4000 m wide DAL shows similar characteristics as these ancient landslides, being steep at the upper part and the foot, and having gentle step-like terraces in the middle part (Figure 2 and Figure 3) (Jones 1993; Dewitte et al. 2006; Panek et al. 2009; Jiao et al. 2013).

The sliding plane of the DAL at 2100 m asl., was inferred from a thin layer of fine grained soil within the intact rock mass on the right slope of the Siweng Gouge exit. The further interlayers which were distributed sporadically on the left bank slope indicated that the DAL had, at one point, dammed the Shuiluo River and thereafter breached quickly. Considering the seismicity of this area, together with the existence of two escarpments, it seems that the DAL slid twice due to a combination of large earthquake and or precipitation during the Quaternary Pleistocene. A few exploratory holes were drilled at a maximal depth of 100 m to find the sliding plane of the DAL, but this was unable to be confirmed, although fragmental quasi-lamellar tuff rock was located at 36 - 64 m in depth (Figure 5).

4. Field investigation and deformation of the DRL

4.1 Basic geological information of the DRL

Within the DAL, the width of the DRL source zone along the river is 1200 m, the length is 420 m, the area is 300,000 m^2 and the estimated volume is 6 million m^3 (Figure 3 and Figure 4). The head scarp is at 2310 m asl. and toe at 2115 m asl., resulting in 195 m elevation difference and an average gradient of 28° for this near-planar, translational slide. The chair-shaped rear scarp subsidence is approximately 40 m - 60 m (Figure 3 and Figure 6). As shown in Figure 6, the long tensile cracks at the rear and the shear cracks at the lateral boundary make the surface water and rainfall easily infiltrate into the slope.

4.2 Destruction and deformation characteristics of the DRL

Between the years 2011 and 2012, tension and shear cracks appeared and developed near the headscarp and the lateral boundary, respectively. Furthermore, bulging of a retaining wall at the toe of the DRL, collapse of the ancillary road slope and small brittle fractures on the bridge were observed (Figure 6). All the failure signs indicated the occurrence of an active landslide (Dong et al., 2015). To try to prevent further deformation, some supporting systems (steel arch and shotcrete-bolt) on the road slope at the hairpin bend were installed in December 2011, but these did not produce the desired effect. From 2012 to 2014, the situation got worse, and many fractures on the top and bottom surfaces of the bridge abutment emerged, putting its operation in danger.

Figure 7, which was taken after the landslide reactivity (20 Dec. 2012), shows that the main scarp subsided a further 3 - 5 m during one month, the arc tension cracks retreated 200 - 2000 mm, and shear cracks extended 50 - 200 mm to the southeast boundary.

In consideration of morphological rupture features and the destruction of engineering works, we concluded that the sliding surface was fully formed by the end of 2012 and the DRL was in an intense

or accelerated deformation stage. If no effective measures were implemented immediately, the threat to the stability of the Dongla Bridge would lead to its destruction (Grana and Tommasi, 2013).

4.3 Deformation characteristics and damage of the Dongla Bridge

Dongla Bridge is a 134 m long and 6.5 m wide prestressed concrete continuous box beam bridge with three spans (Figure 8). The interaction between the thrust of the DRL and the resistance of the bridge's piers led to large and complex local deformations. The main deformations included bulging and fracture of the bridge deck, distortion and toppling of Pier 3, and bulging and cracking of the retaining wall behind Pier 2 (Figure 9). Considering the contrast between the deformation of the retaining wall behind Pier 2 and the absence of cracks on the surface of Pier 1 (furthest away from the landslide bank), we inferred that the exit of the sliding plane was at the foundation cap of Pier 2. Until January 2013, the top horizontal displacements of Piers 1, 2 and 3 reached 94 mm, 160 mm and 316 mm, respectively in different directions (Figure 8).

5. Monitoring

The surface movement of the DRL was monitored from 6th November 2012 to 9th April 2014 (spanning the date of transporting the heavy electrical equipment of - 9th May 2013). The internal movement was monitored by inclinometers daily from 4th to 27th September 2013.

5.1 Surface movement monitoring results

Geodetic survey pillars (SM1-SM20) were installed on 6th November 2012 (Figure 4). Before the emergency mitigation, the maximum displacement rate along the sliding direction was approximately 65 mm/day (Figure 10); during the period from the end of installation of the emergency mitigation measures (5th March 2013) (see Section 6) to the beginning of the rainy season (July 2013), the rate decreased to approximately 40 mm/day; during the rainy season (July to October 2013), it drastically

increased to 97 mm/day and then declined to less than 85 mm/day. This indicates that the sliding rate was sensitive to both mitigation engineering works and rainfall (Panek, 2009). The detailed data from twenty surface monitors are shown in Table 2 and Figure 11. According to the time-series deformation data, this type of motion can be classified as a slow, translational landslide in the Cruden and Varnes (1996) scheme as modified by Hungr et al. (2014).

According to the surface cumulative displacement data over one and a half years, we can see that:

1. The displacements of SM1, SM6, SM11 and SM16 at the toe of the DRL were 59 mm – 393 mm, and relatively minimal among the total monitoring points along the centre sliding vector (SM11 had a larger displacement suggesting some local earth movements due to steep topography), which can be attributed to the emergency mitigation described later in Section 7 and Section 8;
2. The displacements of SM5, SM10 and SM15 at the upmost part of the DRL were 4259 mm – 7062 mm, greatest among the total monitoring points along the center sliding vector, and paving the way for better forecasting and prediction of likely landslide behaviour. The phenomena that the upper displacements being larger than at the toe was in accordance with the inclinometer results. The declining trend of surface displacements from the head to the toe of the DRL (Figure 10 and Figure 11) appears to verify the effectiveness of the emergency mitigation to decrease the deformation rate.

5.2 Inclinometer results

Conventional methods to determine the depth of the sliding surface via rock cores were not possible due to the intense dislocation of boreholes by the sliding movement of the DRL. However, inclinometers could both determine the sliding surface, and track the subsurface movement rates within

the landslide, as done effectively elsewhere (Borgatti et al., 2006; Macfarlane, 2009; Jiao et al., 2013; Massey et al., 2013). As shown in Figure 4 and Figure 5, the inclinometer tubes were installed in three boreholes (B04, B05 and B06) by DHT drilling, and 20 surface monitoring points were distributed on the slope. Figure 5 shows the layout of inclinometers IN1, IN2 and IN3 and the surface monitoring points along the central line of landslide (B-B cross-section in Figure 4). The depth of the tuff rocks from IN1 – IN3 are 35.9 m, 55.0 m and 64.2 m, respectively. It can be inferred that the sliding plane of the DRL is at a depth of 17 m to 19.5 m with a slope of 24° (Figure 12). The cumulative displacements at the crown of the inclinometers were 16 mm, 33 mm and 41 mm, respectively, between 4th and 27th September 2013 (Table 3). It should be noted that because of the hesitation of the stakeholder and the long bidding process, the inclinometer monitoring was implemented after the emergency mitigation construction.

Figure 12 shows that: (1) the cumulative displacement and displacement rate at the top of IN3 is larger than at the other two inclinometers; whereas (2) the cumulative displacement and rate of the major sliding plane at IN1 is larger than other two inclinometers. These two observations suggest that: the external factor which triggered the DRL was erosion or degeneration of the toe of slope, resulting in translational movement at the toe, and the overall geomechanical movement mode is "creep - translational sliding" , resulting in additional shearing within the landslide mass above the toe (Stead et al. 2006; Zhao et al. 2015). This meant that, even though the emergency mitigation at the toe of the landslide did reduce the surficial deformation to some degree, via the reduction in translational movement, the sliding still went on due to shearing. These phenomena illustrate why movements were constantly active and could easily be accelerated.

5.3 Piezometer results

Three piezometers, P1, P2 and P3, were installed at the bottom of the boreholes (B06, B05 and B04) (Figure 4 and Figure 5), corresponding to the location of IN1, IN2 and IN3 respectively. The Darcian permeability coefficient, k, of the chaotic landslide deposits was found to be 1.0 - 1.4×10^{-3} m/s (~ 80-120 m/day). This high value indicates that any groundwater flowing in the landslide would be highly influenced by the river and recent precipitation. However, the observed groundwater level from piezometers readings was determined as about 2110 m, 2115 m and 2125 m asl., respectively, which is located beneath the sliding plane. Therefore, it would have little effect on landslide reactivation. It was assumed that the groundwater level would rise by the same height with the variation of the river water level from the nature condition to the flood condition, as later discussed in Section 7.

6. Emergency mitigation construction of the DRL

Mitigation of hazards of large, deep, and relatively fast-moving landslides is a difficult engineering task, which requires a good understanding of the causes and mechanisms that lead to slope failure (Pulko et al. 2012). In China, applying a surcharge to the toe of the landslide had previously successfully prevented similarly reactivated fossil landslides induced by manmade excavation (Popescu 2001; Li et al. 2006; Picarelli 2011; Chen et al. 2015). Here this method was applied to decrease the sliding rate of the DRL to guarantee the transportation of the heavy electrical equipment and the electric power delivery work as scheduled. 80000 m^3 gunny bags filled with soil were placed at the toe of the DRL, and an artificial slope of 200 m length was thereafter constructed along the Shuiluo River (Figures 13 - 15).

The artificial slope was constructed between 4th and 20th February, 2013, resulting in a satisfactory reduction in the sliding rate (Figure 11), such that the cracks in soil stopped widening, as inspected visually. On 9th May 2013, nine vehicles carrying the heavy electrical equipment with a total load of

1400 kN passed over the Dongla Bridge. The real-time monitoring showed that, in the process of transportation, the bridge structure produced no abnormal displacement (Dong et al. 2014). Moreover, in the period between 3rd and 28th September 2013, the landslide movements by inclinometers decreased to an average value of less than 6 mm / day.

7. Stability evaluation of the DRL

In China, due to its conceptual clarity, versatility and simple calculation process, the Limit Equilibrium Method (Bromhead, 1992) is widely used in slope survey and design, and is specified as the stability evaluation method to be used in general by the China Geological Survey (2006). It should be noted, however, that this method is not suitable when dealing with some special landslides, such as lateral spreads, diffuse landslides, plastic - flow and the rockslide undergoing sudden brittle fracture (Arief et al. 1998; Mendjel and Messast 2012). The crucial prerequisites of this method are that the sliding plane has been determined, the soil of the rupture surface observes a Mohr - Coulomb failure criterion and the sliding body is coherent during sliding. According to the inclinometer monitoring results, the DRL with its planar sliding surface could basically maintain coherence during the sliding stage. Hence, the Limit Equilibrium Method was considered suitable for determining the stability of the DRL, and the calculation accuracy was sufficient to meet the needs of engineering design.

Selection of shear strength parameters is key to accurate determination of stability. Practically speaking, due to the heterogeneity and diversity of the rock and soil mass, it can be difficult to obtain appropriate parameters from testing. The back-calculation procedure presents a relatively easy way to do this, particularly when slopes are under incipient or on-going failure. In practice, some significant status information of the landslide should be considered carefully, including deformation and failure characteristics, field monitoring data etc. From experience, Chinese geologists have empirically

determined a sound relationship between the calculated stability coefficient of the slope (also known as the Factor of Safety against sliding (Bromhead, 1992)) and such the status information, that includes deformation and failure characteristics, as well as monitoring data (Table 4). Because the deformation of DRL and initial damage of Dongla Bridge appeared just after the slope excavation, it was hypothesized that the DRL had been stable and was at the limit equilibrium state (stability coefficient = 1) before the excavation.

The natural and saturated densities of the silty clay soil were obtained from laboratory testing as 1960 kg/m^3 and 2150 kg/m^3, respectively. Based on the most conservative considerations, the frictional resistance parameters were obtained from back analysis (Table 5) using the Limit Equilibrium Method.

The integral stability coefficients of the DRL were calculated under three scenarios with two water levels (Table 6 and Figure 16), which shows that the DRL would be unstable under both rainfall and earthquake conditions.

8. Reactivity mechanism of the DRL

As for most large-scale ancient landslides, the deposit usually deforms with gravitational creep (Cui et al. 2008). When it comes to the reactivity of ancient landslides, a large number of cases indicate that the new-forming sliding planes tend to occur along pre-existing rupture surfaces, which are normally interfaces between rock and soil (Dai et al. 2000; Dewitte et al. 2006). Significantly, the formation mechanism of the rupture surface is sensitive to environmental changes and human disturbance (Jones et al. 1993; Dai et al. 2000).

As far as the DRL is concerned, a comparative analysis of geomorphic characteristics and the pattern of sliding plane can provide insight into the revival mechanism. Firstly, by comparing to the stable region within the DAL, it is inferred that precipitation and fluvial incision by the river are not the main

destabilizing factors. Secondly, it is noted that the gol mining pits were predominantly located in the DRL. It is thought that their deterioration could fracture the soil texture and accelerate the creep speed of the DRL (Benko and Stead, 1998). Thirdly, because the sliding plane of the DRL was 1) evolving throughout the soil layer over a depth of approximate 19.5 m, and 2) planar and therefore different from such arc-shaped landlside triggered in homogeneous soils, a relatively rapid external environmental changes, such as the modification of the surficial geometry via toe removal, could be ultimately responsible for the reactivaton.

In this regard, it is inferred that the revival mechanism of the DRL is an accelerated creeping - translational sliding triggered by initial gold mining and subsequent slope-cutting construction. The declining trend of the surface displacements after the emergency mitigation (Figure 10) also appears to verify this analysis. Therefore, the construction on previously mined slope should be carefully considered, or else, avoided a similar situation in the future.

9. Analysis on the development trend of the DRL and cascading hazards

Although the sliding rate of the DRL was decreased by the emergency mitigation, the displacement still increased slowly. In Februry 2014, a number of tensile cracks emerged on the artificial slope, presenting a potential risk to the stability of the bridge (Figure 17). Although the landslide would not be expected catastrophically accelerate under the state of low-speed deformation (Picarelli 2011), a sudden increase of the driving force (due to an inundation, heavy preciptation, or earthquake, etc.) could still lead to the destruction of the bridge. In the worst case scenario, river blockage or surge generation could happen because of the volume, location and activity of the DRL (Macfarlane 2009). Considering the volumes involved, in the worst case scenario where the moving mass slid coherently in wholly translational sliding, it could block the Shuiluo River and form a landslide dam with a

calculated maxium height of 20 m in accordance with the thickness of the sliding body. Considering the 5% river bed gradient of the Shuiluo River, it might cause a backward length of impounded water of about 400 m and a lake capacity about 0.4 million m^3. According to local geological experience, due to the fast rise of impounded water, the loose barrier materials would easily be breached in a short period and form a debris flow (Xu et al. 2013; Liu et al. 2010). The largest downstream peak flow was speculated to be 1400 m^3/s reaching 10 km downstream, but it would not be expected to exceed the conveyance capacity of this segment of Shuiluo River (Table 7). If, on the other hand the DRL were ruptured internally and fell block by block into the river, the blocks would easily be washed away. In this case, the travel distance and covered area would be much more limited (Eberhardt et al. 2004).

10. Future options

Large ancient landslides in mountainous regions are vulnerable and liable to be reactivated by environmental changes such as changes of hydrologic balance and climate (Panek 2009). It is of utmost importance that any active mitigation measures are designed not only to efficiently restrain the sliding mass, but also to guarantee safe construction, with the likelihood of damage reduced to an acceptable level during the construction process (Pulko et al. 2012). Based on this consideration, several permanent treatment solutions for the DRL were proposed. However, to simply stabilize the sliding zone at the ancillary road section would cost nearly 100 million yuan, which would be unrealistic. In fact, the proprietor was in the dilemma of whether sustaining the existing Dongla Bridge with stabilization construction, which would be expensive and probably useless in the long term under the complex geological condition, or establishing a new bridge instead. After comprehensive comparison, the second plan was adopted. Thus the old bridge was dismantled via a controlled explosion (Figure 18), and a site to build the new bridge was chosen downstream outside the DAL. In the meantime, the

observation of the DRL is still being undertaken to avoid potential landslide hazards.

11. Conclusion

This paper has discussed the investigation, monitoring, analysis and mitigation of a large translational creeping landslide, affecting an important infrastructural activity in a remote and mountainous region in China. By doing so, the study examined a range of possible triggers and scenarios that could lead to the instability and therefore considered a series of options to enable engineering works to proceed. As a case study, it illustrates how engineers and geologists can pragmatically approach a most complex and potentially dangerous situation by the judicious use of relatively simple engineering tools, such as site investigation, Limit Equilibrium analysis, back analysis and monitoring.

The Dongla Reactivated Landslide - a partially reactivated portion of the Dongla Ancient Landslide, was reactivated in June 2011, resulting in a direct threat to the security and serviceability of the Dongla Bridge. As the vital transportation of heavy electrical equipment across the Dongla Bridge had been scheduled on 9 May 2013, ensuring the stability and security of the bridge became a primary emergency task. In order to achieve this goal, detailed field surveys and mapping were first completed to obtain a delineation of the DRL. Subsequently, surface displacement monitoring was carried out, from the November 2011 to April 2014, to provide data for the evaluation of the trends in movement, and the internal deformation was monitored by inclinometers every day to determine the sliding plane and stage of deformation. The installation of such inclinometers were key to determining the location of the sliding plane of the DRL and their continuous monitoring enabled the effect of time to be ascertained (i.e. whether the slide was accelerating, steadily moving or decelerating); the efficacy of the

mitigation measures (i.e. did the arrest or slow the landslide); and the role of water (i.e. how was the rate of sliding affected by rainfall).

The result showed that the DRL is an accelerated creeping - translational slide, located with the fractured and sheared material of the much larger DAL. Consideration of local history, ground survey and observations of the timing of slope movement led to the conclusion that the DRL was triggered by initial gold mining and subsequent slope-cutting construction. It was the combination of such investigative activities that enabled a full scenario to be postulated.

Based on the subsequent stability analysis and on geological experience, emergency mitigation measures were implemented at the toe of the slide from January 2013 to March 2013. Considering the remote location of the landslide, the implementation of further mitigation measures, such as the use of large concrete shafts along the slide as applied elsewhere (e.g. Pulko et al. 2012), was not considered feasible in terms of economic cost versus benefit. However, according to the monitoring data of the surface movement of the DRL, the toe mitigation reduced the sliding rate of the landslide effectively to enable the transportation of the heavy electrical equipment in a timely manner.

This study has provided an insight into the problems associated with the interaction between engineering construction and the dynamic behavior of a reactivated and rapidly moving translational landslide. Further, the emergency mitigation mentioned in this paper is worth noting as a potentially effective method to temporarily stabilize reactivated landslides caused by human activities. Conclusively, for similar fragile mountain environments, the consideration of future engineering projects along river banks should follow a detailed ground survey and geotechnical investigation, coupled with an examination of possible future scenarios including groundwater movement, seismic activity, and the influence of human activities.

12. **Acknowledgements**

This work was supported by the National Natural Science Foundation of China (Grant nos. 41402266 and 41672283), the Fundamental Research Funds for the Central Universities (Project No. 2682015CX011), and the China National scholarship fund for academic visitors. We also would like to express our gratitude to Yang Guan form Southwest Electric Power Design institute Co.Ltd. for his kind assistance in the field and Zhongpan Shu from Sichuan Institute of Geological Engineering Investigation for providing the monitoring data.

References

Arief S, Adisoma G, Arif I (1998) Fast and efficient procedures for stability analysis using generalized limit equilibrium method. Proceedings of the International Symposium APCOM: 123-129.

Benko B, Stead D (1998) The Frank slide: a reexamination of the failure mechanism. Canadian Geotechnical Journal 35(2): 299-311. doi:10.1139/t98-005

Borgatti L, Corsini A, Barbieri M, Sartini G, Truffelli G, Caputo G, Puglisi C (2006) Large reactivated landslides in weak rock masses: a case study from the Northern Apennines (Italy). Landslides 3(2): 115-124. doi: 10.1007/s10346-005-0033-9

Bromhead EN (1992) The Stability of Slopes Blackie Academic and Professional. GB.

Chen XP, Zhu HH, Huang JW, Liu D (2015) Stability analysis of an ancient landslide considering shear strength reduction behavior of slip zone soil. Landslides: 1-9. doi:10.1007/s10346-015-0629-7

China Geological Survey (2006) Specification of Design and Construction for Landslide Stabilization (DZ/T0219-2006). China Standard Press, Beijing.

Cui J, Wang LS, Xu J, Wang XQ, Yao Q (2007) Stability analysis of old landslide for a possible ancient landslide event blocking middle of Jinsha river. Journal of Engineering Geology 16(1): 6-10. (In Chinese)

Dai FC, Chen SY, Li ZF (2000) Analysis of landslide initiative mechanism based on Stress-strain behavior of soil. Chinese Journal of Geotechnical Engineering 22(1): 127-130.

Dewitte O, Chung CJ, Demoulin A (2006) Reactivation hazard mapping for ancient landslides in West Belgium. Natural Hazards and Earth System Sciences 6(4): 653-662. doi:10.5194/nhess-6-653-2006

Dong JH, Tang XL, Shu ZP, Li DX (2014) Study on mechanism of reactivation and its stability in Dongla landslide, Shuiluo town, Muli city. Journal of Engineering Geology 122-129. (In Chinese)

Dong JH, Wei LS, Tang R, Li DX, Deng R (2015) Safety monitoring and deformation damage of Dongla landslide in Shuiluo of Muli County. South-to-North Water Transfers and Water Science & Technology 13(3): 543-547. (In Chinese)

Eberhardt E, Stead D, Coggan JS (2004) Numerical analysis of initiation and progressive failure in natural rock slopes—the 1991 Randa rockslide. International Journal of Rock Mechanics and Mining Sciences 41(1): 69-87. doi:10.1016/S1365-1609(03)00076-5

Grana V, Tommasi P (2013) A deep-seated slow movement controlled by structural setting in marly formations of Central Italy. Landslides 11(2): 195-212. doi:10.1007/s10346-013-0384-6

He JL (2005) Estimating of the landslide stability and fatalness cause of earthquake in Muli in the Szechwan the

province. Engineering master degree thesis of Southeast Jiaotong Unversity 1-141. (In Chinese)

Huang RQ (2015) Understanding the Mechanism of Large-Scale Landslides. Engineering Geology for Society and Territory. Landslide Processes 2: 13-32.

Jiao YY, Wang ZH, Wang XZ, Adoko AC, Yang ZX (2013) Stability assessment of an ancient landslide crossed by two coal mine tunnels. Engineering Geology 159(11): 36-44. doi:10.1016/j.enggeo.2013.03.021

Jiang ZX (2013) Outline of engineering design for post-earthquake disaster management in Mountainous Region. Southwest Jiaotong University Press. Chengdu (In Chinese)

Jones PB (1993) Structural Geology of the Modern Frank Slide and Ancient Bluff Mountain Slide, Crowsnest, Alberta. Bulletin of Canadian Petroleum Geology 41(2): 232-243.

Li XZ, Kong JM, Xu Q (2006) Deformation and Development Tendency of Shiliushubao Landslide by Numerical Modeling. Wuhan university journal of natural siences 11(4): 840-846.

Liu N, Chen Z, Zhang J, Lin W, Chen W, Xu W (2010) Draining the Tangjiashan barrier lake. Journal of Hydraulic Engineering 136(11): 914-923. doi:10.1061/(ASCE)HY.1943-7900.0000241

Macfarlane DF (2009) Observations and predictions of the behaviour of large, slow-moving landslides in schist, Clyde Dam reservoir, New Zealand. Engineering Geology 109(1-2): 5-15. doi:10.1016/j.enggeo.2009.02.005

Massey CI, Petley DN, McSaveney MJ (2013) Patterns of movement in reactivated landslides. Engineering Geology 159(12): 1-19. doi:10.1016/j.enggeo.2013.03.011

Mendjel D, Messast S (2012) Development of limit equilibrium method as optimization in slope stability analysis. Structural Engineering and Mechanics 41(3): 339-348. doi: 10.12989/sem.2012.41.3.339

National Seismic Standardization Technical Committee (2015) Seismic ground motion parameters zonation map of China (GB18306-2015). China Standard Press, Beijing.

Panek T, Hradecky J, Silhan K (2009) Geomorphic evidence of ancient catastrophic flow type landslides in the mid-mountain ridges of the Western Flysch Carpathian Mountains (Czech Republic). International Journal of Sediment Research 24(1): 88-98. doi:10.1016/S1001-6279(09)60018-4

Picarelli L (2011) Discussion to the paper “Expected damage from displacement of slow-moving slides” by M.F. Mansour N.R. Morgenstern and C.D. Martin. Landslides 8(4): 553-555. doi:10.1007/s10346-011-0292-6

Popescu ME (2001) A suggested method for reporting landslide remedial measures. IAEG Bull 60(1): 69–74. doi:10.1007/s100640000084

Pulko B, Majes B, Mikoš M (2012) Reinforced concrete shafts for the structural mitigation of large deep-seated landslides: an experience from the Macesnik and the Slano blato landslides (Slovenia). Landslides 11(1): 81-91. doi:10.1007/s10346-012-0372-2

Stead D, Eberhardt E, Coggan JS (2006) Developments in the characterization of complex rock slope deformation and failure using numerical modelling techniques. Engineering Geology 83(1-3): 217-235. doi:10.1016/j.enggeo.2005.06.033

Wang GL, Zhang YX, Wen HJ, Chen HP (2003) Analysis on deformation characteristic sand formation of revived fossil landslide in Daheba. Journal of Chongqing Jianzhu University 25(5): 1-4. (In Chinese)

Wei ZA, Yin GZ, Wang JG, Wan L, Jin LP (2012) Stability analysis and supporting system design of a high-steep cut soil slope on an ancient landslide during highway construction of Tehran-Chalus. Environmental Earth Sciences 67(6): 1651-1662. doi:10.1007/s12665-012-1606-2

Xu WJ, Xu Q, Wang YJ (2013) The mechanism of high-speed motion and damming of the Tangjiashan landslide. Engineering Geology 157(6): 8-20. doi:10.1016/j.enggeo.2013.01.020

Zhao Y, Xu M, Guo J, Zhang Q, Zhao H, Kang X, Xia Q (2015) Accumulation characteristics, mechanism, and identification of an ancient translational landslide in China. Landslides 12(6): 1119-1130. doi:10.1007/s10346-014-0535-4

Table 1 Grain-size distribution of the surficial landslide deposit

Material	Color	Grain-size (mm)	Finer by mass (%)
clay and silt	yellowish	< 0.075	25
sand	yellowish-brown	0.075 - 2	40
gravel	blue-grey	2 - 20	70
block	blue-grey	20 - 200	100

Table 2 the surface cumulative displacement monitor result (6 Nov. 2012 – 9 Apr. 2014)

Surface Monitor	X direction (mm)	Y direction (mm)	Z direction (mm)	Surface Monitor	X direction (mm)	Y direction (mm)	Z direction (mm)	Surface Monitor	X direction (mm)	Y direction (mm)	Z direction (mm)
1	393	-107	-29	8	3089	-209	-504	15	7063	-1587	-3767
2	334	-24	-334	9	5234	-921	-2804	16	149	39	-92
3	1362	59	-507	10	6381	-1490	-3568	17	10	-18	4
4	3890	-574	-1738	11	2272	-1029	-885	18	6837	-2020	-4352
5	4260	-1296	-2956	12	3170	-1020	-1871	19	7026	-1860	-4328
6	59	-4.2	-17	13	62170	-1113	-1468	20	6051	-1100	-4463
7	1528	-548	-815	14	6183	-171	-2878				

Note that: X represents the sliding direction; Y is perpendicular to the X direction towards upstream; Z represents the vertical direction (gravity direction).

Table 3 Summary of inclinometer results (04.09.2013～27.09.2013, when the inclinometers were assumed to shear during landslide movement)

Inclinometer	Depth of borehole	Depth of sliding surface	Cumulative displacement at top of inclinometer tubes	Mean displacement rate at top of inclinometer tubes	Cumulative displacement of sliding plane	Displacement rate of sliding plane
	(m)	(m)	(mm)	(mm/day)	(mm)	
IN1	60.0	18.5	16	0.7	14	0.6
IN2	70.4	19.5	33	1.9	3	0.7
IN3	100.4	17.0	41	5.9	-	-

Table 4 Relationship between developed stage and stability coefficient (Jiang, 2006)

Developed stage	Surface deformation	Maximal displacement of sliding plane	status of sliding plane	Stability coefficient
Embryonic stage	Invisible	Millimeter	-	≥ 1.1
Creep stage	Deformation evidence at scarp and toe	Centimeter	Coalescence of fractures / at limit equilibrium state	1.0 – 1.1
Sliding stage	mainscarp subsidence and toe bulge	Decimeter - meters	Wholesale rupture and complete failure	0.95 – 1.0
Emplacement stage	Sedimentation, partial collapse	-	-	≥ 1.0

Table 5 Physical and mechanical parameters of the sliding belt

parameters of surface of rupture		Dry or wet	density (kg/m^3)	Cohesion (kPa)	Internal frictional angle (°)
natural state	Value from BCA	D	1960	7.0	24.3
rainfall state	Value from BCA	W	2150	7.0	22.8

Table 6 Stability coefficients of the DRL under different scenarios

Sliding plane	Water lever of river	Scenarios	Stability coefficient	Stable state
1	Normal	Normal	1.05	basic stable
		Rainstorm	0.88	Unstable
		Earthquake	0.99	Unstable
	Flood	Normal	1.03	basic stable
		Rainstorm	0.87	Unstable
		Earthquake	0.97	Unstable
2	Normal	Normal	1.02	basic stable
		Rainstorm	0.85	Unstable
		Earthquake	0.95	Unstable
	Flood	Normal	1.00	basic stable
		Rainstorm	0.84	Unstable
		Earthquake	0.94	Unstable

Table 7 Influence on downstream after dam-breaking

item	The position downwards barrier dam (m)						
	0 (dyke breach)	200	500	1000	2000	5000	10000
Peak flow（m^3/s）	2318	1933	1639	1540	1494	1451	1429
Height of flood crest (m)	21.8	15.5	13.4	12.7	10.7	7.7	3.2

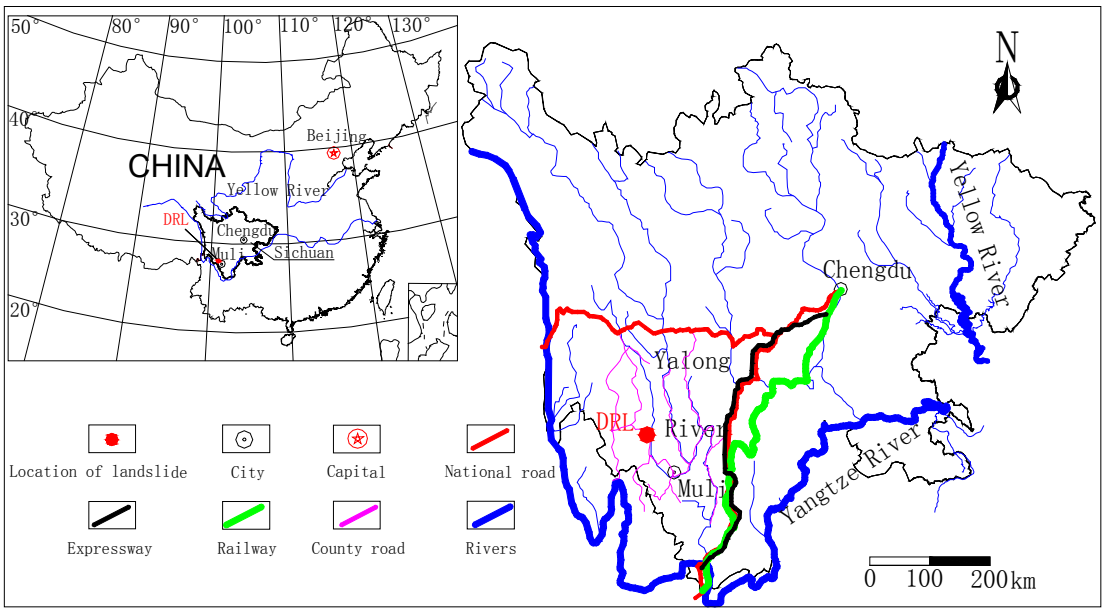

Fig. 1. Location of Dongla Reactivated Landslide (DRL) and its nearby cities and towns.

Fig. 2. Delineation of the Dongla Ancient Landslide and Dongla Reactivated Landslide.

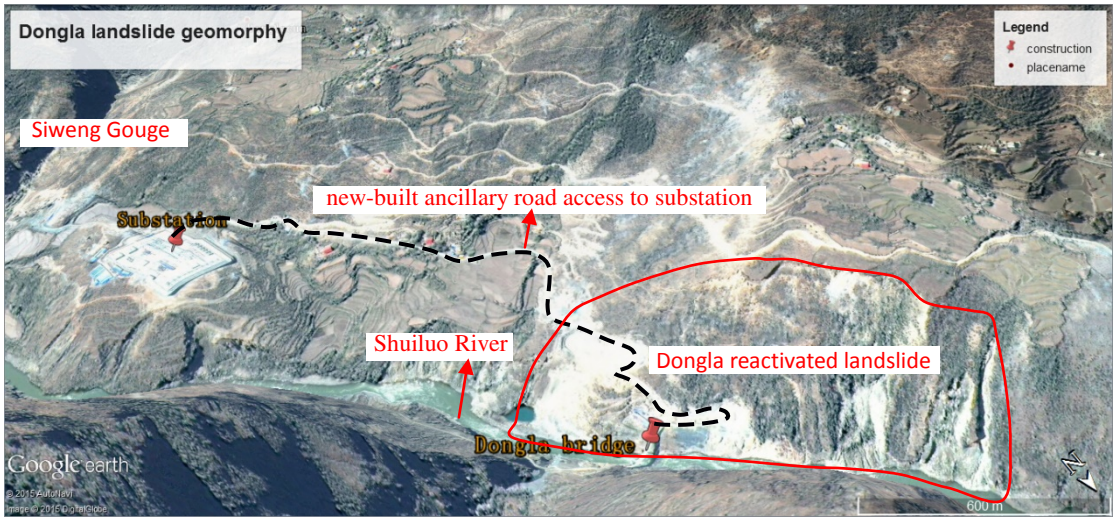

Fig. 3. Location of the Dongla Bridge and Dongla Reactivated Landslide. The construction of the Dongla Bridge and the new ancillary road (black line), as well as the gold mining pits and the gold washing pond destabilized the slope.

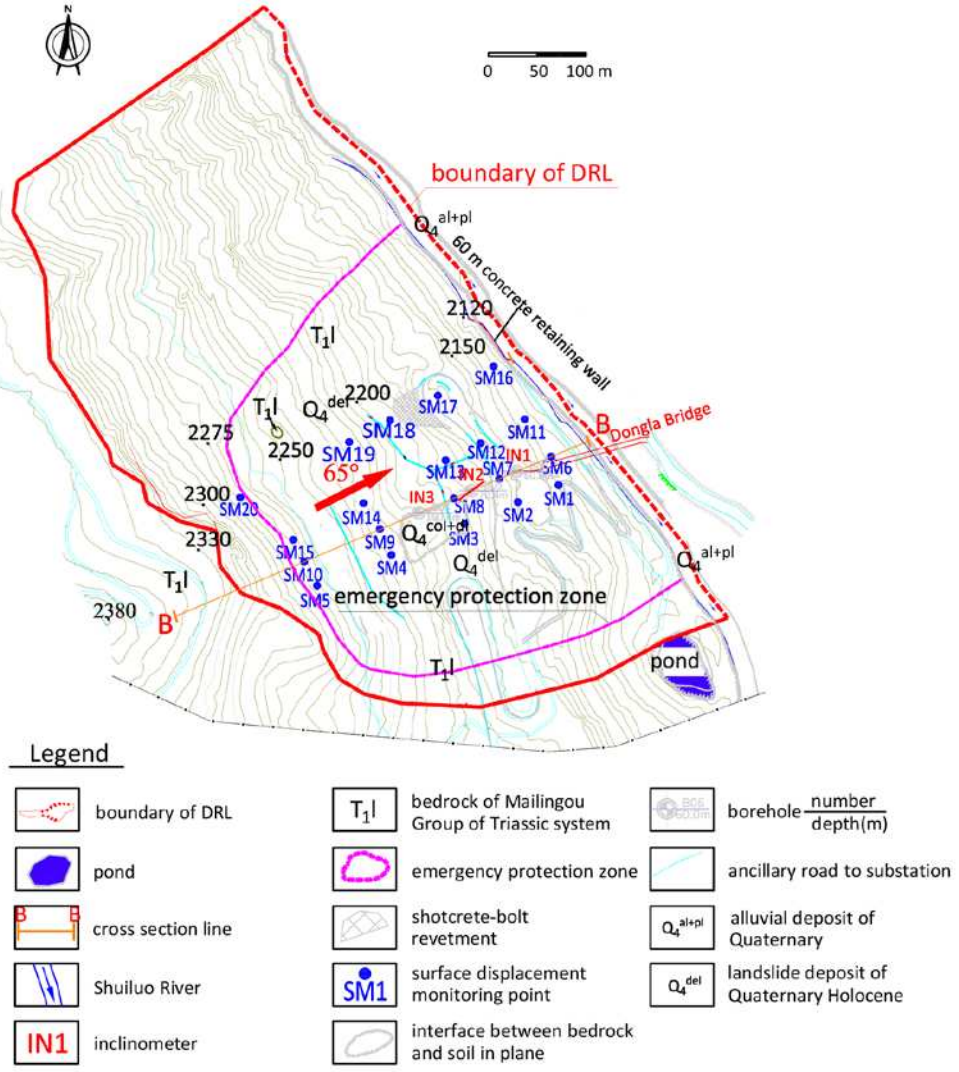

Fig. 4. The engineering geological plane and the arrangement of displacement monitoring points of the DRL (inclinometers IN1 – IN3: red; surface monitoring points SM1 – SM20: blue).

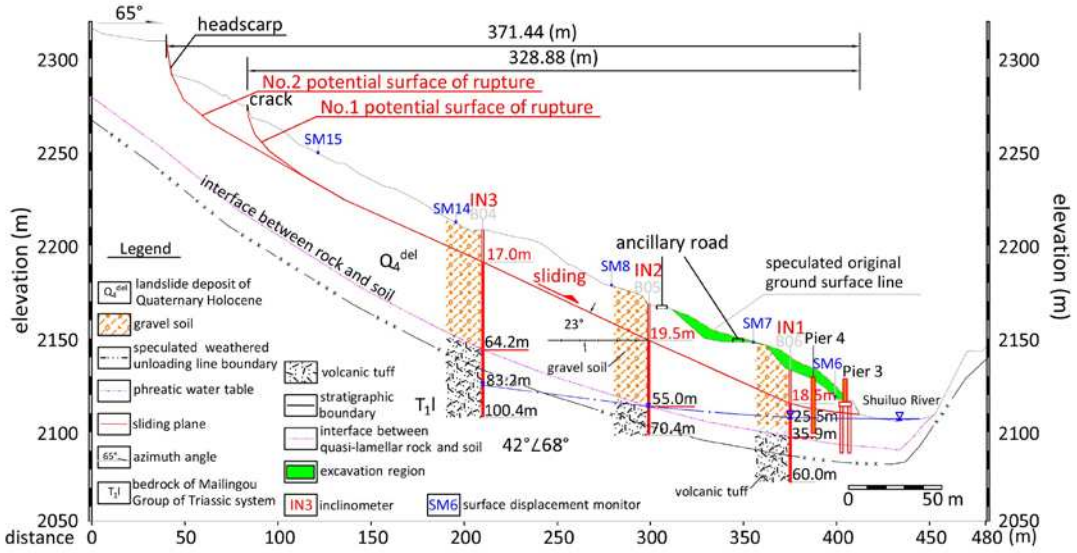

Fig. 5. The monitoring deployment on the geological cross-section (B-B) of the DRL. IN1 – IN3 represent the inclinometers, SM6 – SM10 represent the surface displacement monitors.

Fig. 6. Main scarp and local deformation features of the DRL. Viewing towards southwest.

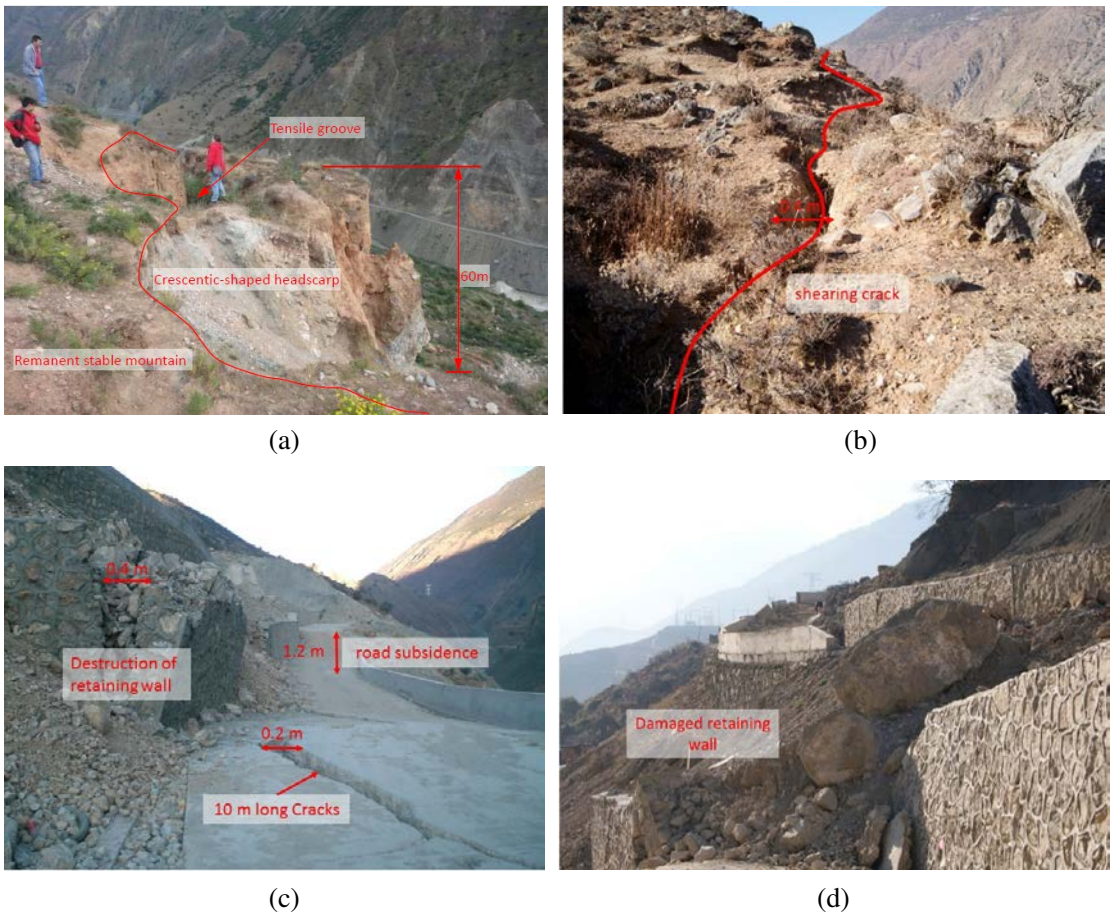

(a) (b)

(c) (d)

Fig. 7. Deformation evidence: (a) 60 m Headscarp of the DRL, viewing north; (b) 380 m long and 0.1 - 0.4 m wide twisty right shearing crack of the DRL mainly cut through the soil; (c) damage of retaining wall and ancillary road pavement; (d) subgrade failure of the ancillary road.

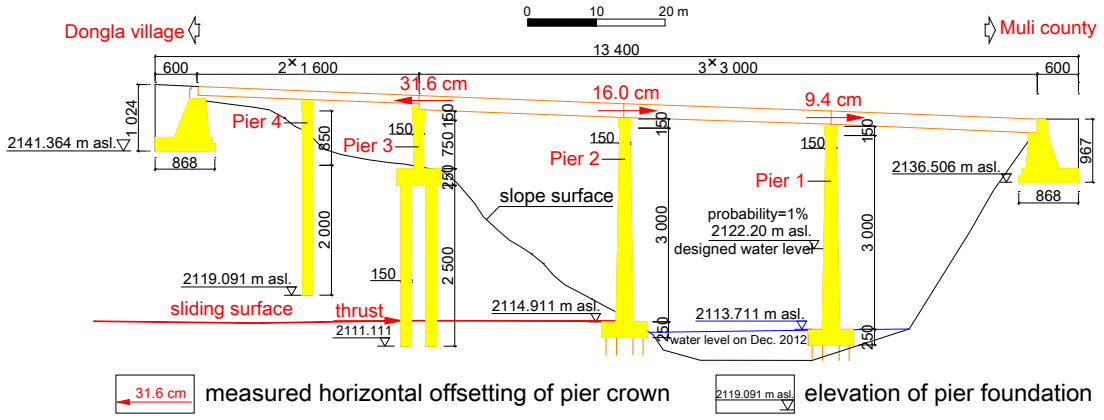

Fig. 8. Displacements of the Dongla Bridge's piers and structure of the bridge (elevation unit:m; other unit:cm; red arrow indicating the direction of pier's displacement and thrust of the DRL) (modified after Wang, 2013).

(a)

(b)

(c)

Fig. 9. Damage to bridge abutment and dislocation of bridge deck slab (a) Crack of west abutment. (b) burial cracks on the back surface of Pier 2. (c) deformation of Pier 3.

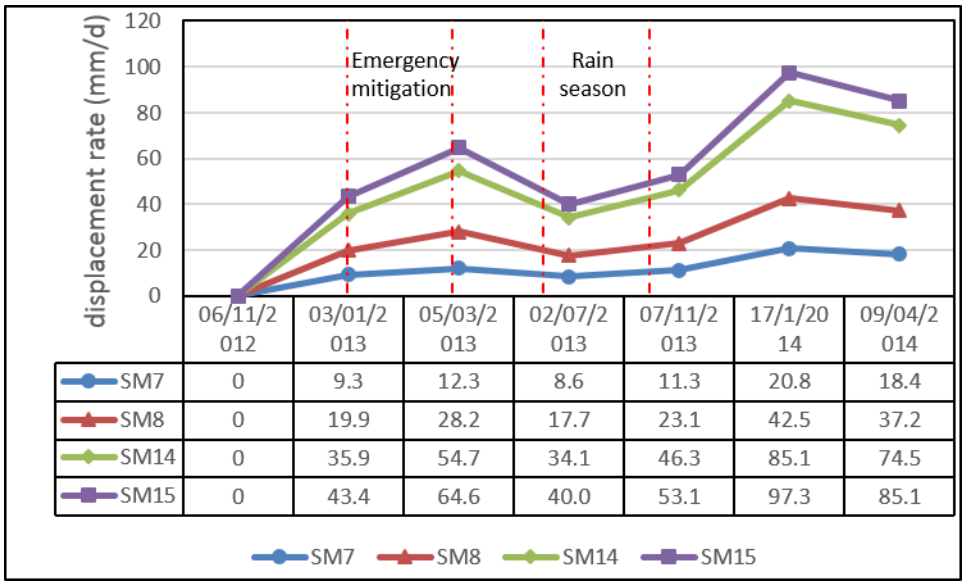

	06/11/2012	03/01/2013	05/03/2013	02/07/2013	07/11/2013	17/1/2014	09/04/2014
SM7	0	9.3	12.3	8.6	11.3	20.8	18.4
SM8	0	19.9	28.2	17.7	23.1	42.5	37.2
SM14	0	35.9	54.7	34.1	46.3	85.1	74.5
SM15	0	43.4	64.6	40.0	53.1	97.3	85.1

Fig. 10. The displacement rate of four surface monitoring points along the center cross section B-B.

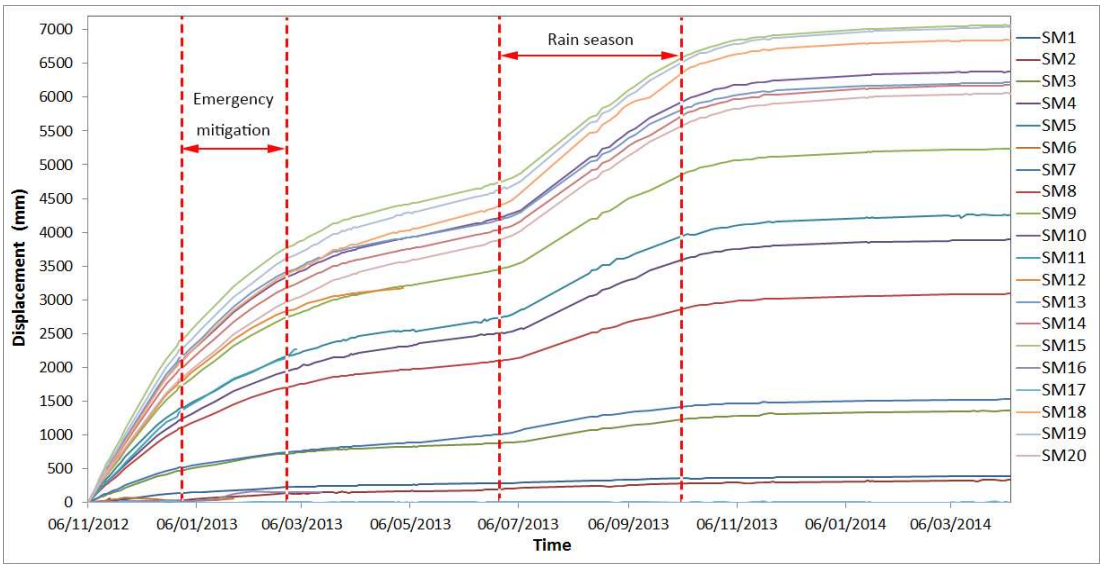

Fig. 11. The surface movement monitoring result. The displacement vector is consistent with the sliding direction.

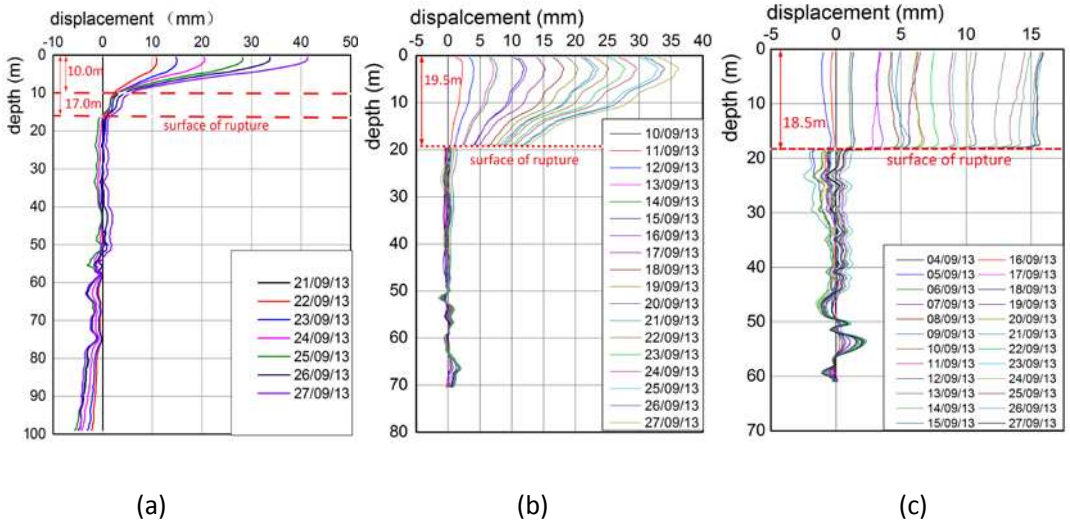

(a) (b) (c)

Fig. 12. Cumulative horizontal displacement vs the depth of inclinometers along the sliding vector (a) IN1 (b) IN2 (c) IN3 from 1st to 27th September 2013.

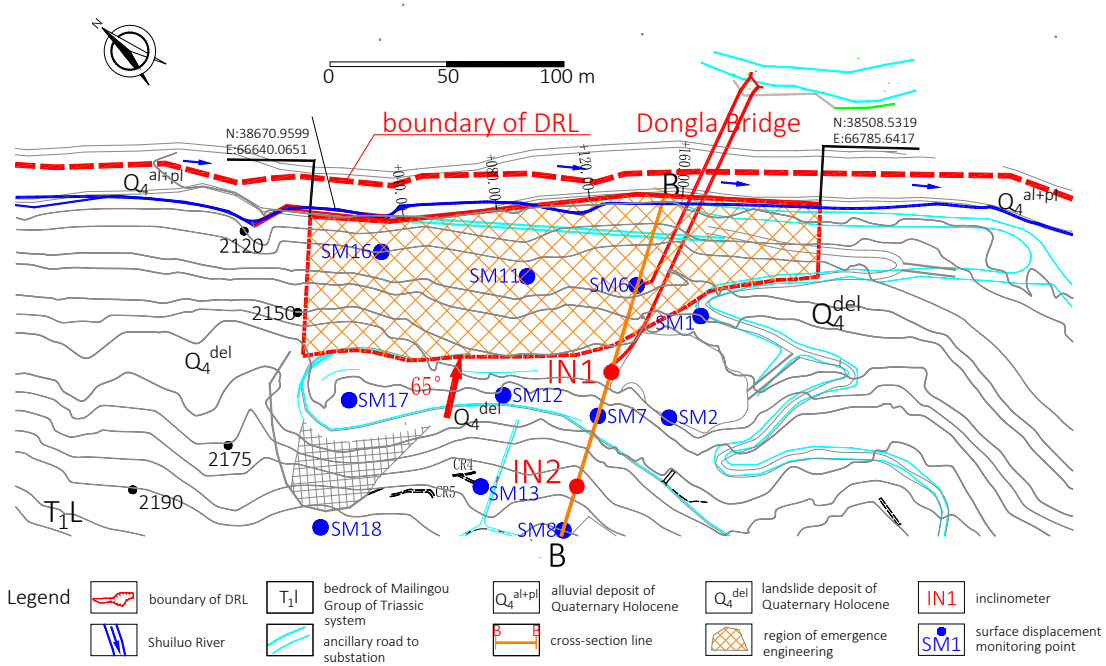

Fig. 13. Layout of emergency mitigation engineering of the DRL.

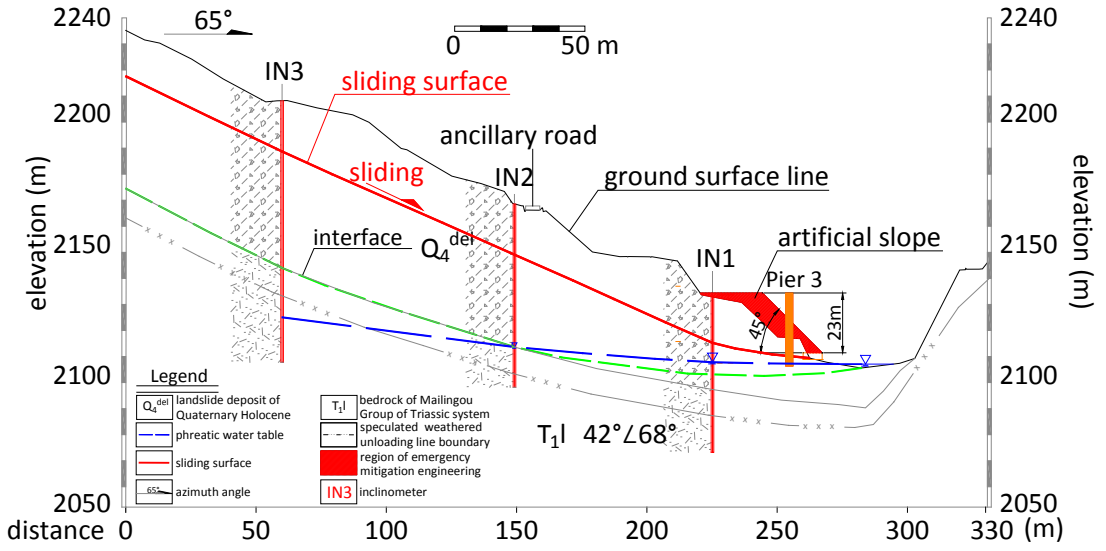

Fig. 14. Emergency mitigation engineering for the DRL (B-B cross-section). The artificial slope was 23 m high and 5 m wide with a gradient of 45°, and was divided into 5 berms with a 5 - 8 m altitude vertical difference between each.

Fig. 15. Artificial slope (photograph taken 12th December 2015).

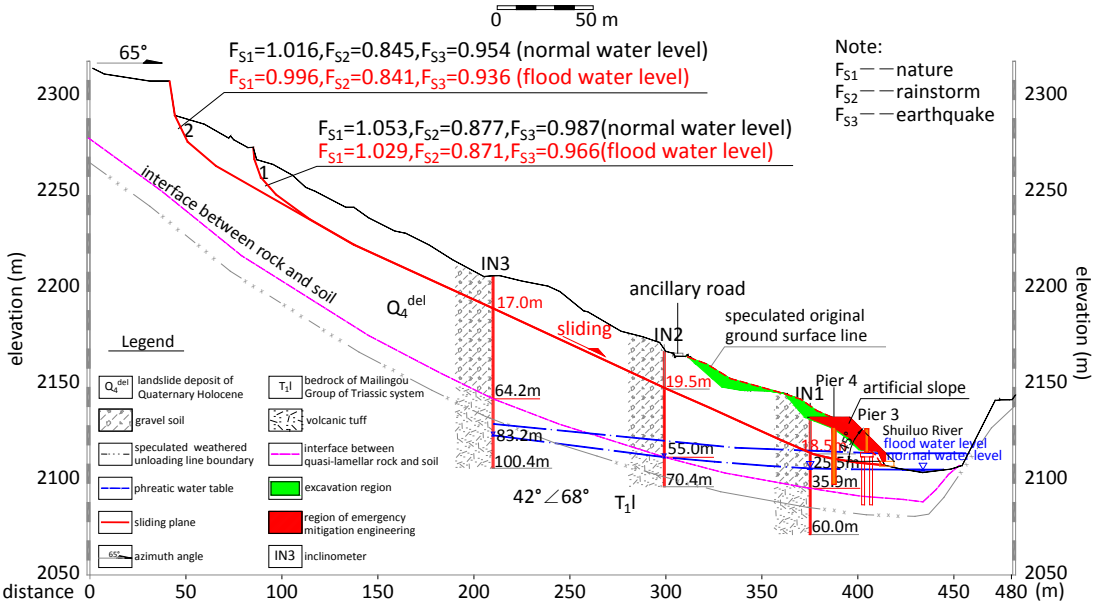

Fig. 16. Stability coefficients of the DRL under different scenarios (cross-section B-B).

Fig. 17. New emerging arc tensile cracks on the artificial slope (photo taken February 2014)

Fig. 18. Dongla Bridge was dismantled by bomb explosion on 12th July 2015.